Spark Plasma Sintering of Biomedical Composite for Orthopedic Applications

Chander Prakash[1]

[1]School of Mechanical Engineering, Lovely Professional University, Phagwara-144411, Punjab, India

Abstract

Here in, a bio-inspired biodegradable Mg-Zn-Mn-Si Alloy was synthesised by mechanical alloying and spark plasma technique. The effect milling time, sintering temperature, and sintering pressure has been studied on the elastic modulus and hardness of the as-synthesized alloy. The microstructure, surface topography, and element composition as-synthesized alloy was investigated using optical microscope, field-emission scanning electron microscopy, and energy-dispersive X-ray spectroscopy. The elastic modulus and hardness of as-synthesized alloy was measured by nano-indentation technique. The microstructure examination of the compact reveled that Si not only refined the gain structure but also formed Mg_2Si in the structure. XRD pattern analysis confirmed the formation of Mg_2Si, Mg-Zn, Mn-Si, SiO_2, and ZnO_2 due to heat developed during the process, which enhanced the mechanical properties and corrosion characteristics.

Keywords: Mg alloy; Mechanical Alloying; Spark plasam Sintering; Microhardness.

1. Introduction

To meet the requirements of joint replacement challenges, the development of various implants material has been witnessed and the need of biomaterials is increasing rapidly [1]. Biomaterial artificial or natural material is used to fabricate the artificial organ or implants to restore the functionality of diseased or dysfunctional natural organ [2]. The biomaterials are categorized as metallic, ceramics and polymers used for the development of various implants as shown in Figure 1.1 [3]. The common metallic biomaterials are stainless steels (SUS-316L), cobalt-chromium (Co-Cr), titanium (Ti) and its alloys [4]. Among these, Ti and its alloys have recently gained increasing attention for application in the biomedical field owing to their superior biocompatibility and excellent mechanical properties [5]. There are some serious weaknesses of the Ti alloys: (1) the elastic modulus of Ti alloys (CP-Ti and Ti-6Al-4V) are much high (110 GPa) as compared to bone (10–45 GPa). This distinct mechanical mismatch of elastic modulus between the implant, the surrounding bone and its tissues will cause stress shielding, which start bone resorption and implant start loosening and results in implantation failure [6-7]; (2) the presence of Al and V restricts the applicability of Ti-6Al-4V because during abrasion, it releases ions and creates cytotoxicity which results in allergic reactions. As a result of this, the implant must be removed from the body by using a secondary surgical intervention and additional surgery causes an increase in costs to the health care system, as well as emotional stress to the patient [8].

Fig. 1. Representative example of application of metallic biomaterials: bone fixation devices

In order to overcome above said drawbacks, the researcher developed biocompatible V and Al-free β-phase Ti alloy such as Ti-Nb, Ti-Zr, Ti-Nb-Zr, Ti-Nb-Ta-Mo, Ti-Nb-Ta-Sn and Ti-Nb-Ta-Zr (TNTZ) alloys [2,4,5, 9-12]. Rrecently developed β-Ti alloys have lower elastic modulus of 55 GPa (comparable with that of bone i.e., ~20 GPa), higher strength, lower density, better corrosion resistance abilities, and superior biocompatibility than commercially pure Ti and Ti-6Al-4V alloys [13-17]. The β-type Ti-33Nb-7Ta-5Zr alloy has been widely used for the fabrication of biomedical implant, due to its unique combination of mechanical properties especially low elastic modulus (55 GPa), non-toxic, excellent biocompatibility and superior electrochemical properties [18-19]. The Nb β-stabilizer reduces the elastic modulus and decreases stress shielding difference between bone and implant, and promotes load sharing [20-22]. The Zr element provide a high level of blood compatibility and the Nb and Ta elements provides a passive oxide film consisting of dense rutile structure on the alloy surface enhanced corrosion properties and bioactivity [23-26].

However, despite their excellent mechanical properties, Ti and its alloys do not effectively meet the requirements of osseointegration that involves efficient binding to surrounding tissues and bone [27]. Thus, to maximize their bioactivity, the surface of Ti-based implants has been modified by depositing a layer of bioactive substance hydroxyapatite (HaP) through mechanical, physical, chemical, or biochemical treatments, which increases the fabrication cost of the implants [2,12,28]. For this reason and in order to avoid secondary treatment, a better fabrication technology for the production of porous bio-compatible structure, low modulus β-type Ti alloys comprising non-toxic and non-allergic elements are urgent needed for the next generation of implants. There are various new fabrication technologies such as laser beam machining, ion beam machining, hot isostatic pressing (HIP) and hot sintering, has been developed and used for the production of porous bio-compatible structure of β-type Ti alloys [29-30]. These techniques produce porous structure, but there long sintering time, temperature weaken the mechanical and electrochemical properties, which failed the implant at cyclic load condition and long term performances. Recently, Spark Plasma Sintering (SPS) technique was used as fabrication technique for the synthesis of porous metallic implants [31]. The SPS technique is a powder metallurgy process, and the consolidation of powders by sintering uses a shorter holding time, a relatively lower sintering temperature, and a high pressure at the rapid heating and cooling rates (>100 ºC/min)

2. Spark Plasma Sintering (SPS)

Sintering is the process of making objects from powder, by heating the material in a furnace below its melting point so that bonding takes place by diffusion of atoms. Conventional electric hot press techniques use DC or commercial AC power, and the principle factors promoting sintering in these techniques are the Joule heat generated via the electricity supply (I^2R) and the plastic go with the flow of materials because of the utility of stress. Whereas, Spark plasma sintering (SPS) or pulsed electric current sintering (PECS) is considered as non-conventional sintering technique utilizing uniaxial force and a pulsed (on-off) direct electrical current (DC) under low atmospheric pressure to perform high speed consolidation of the powder.

2.1. Basic configuration of the SPS system

The system consists of a SPS sintering machine with a vertical single-axis pressurization mechanism, specially designed punch electrodes incorporating water cooler, a water-cooled vacuum chamber, a vacuum/air/argon-gas atmosphere control mechanism, a special DC-pulse sintering power generator, a cooling water control unit, a position measuring unit, a temperature measuring unit, an applied pressure display unit and various interlock safety units. Figure 1 shows the schematic of SPS machine.

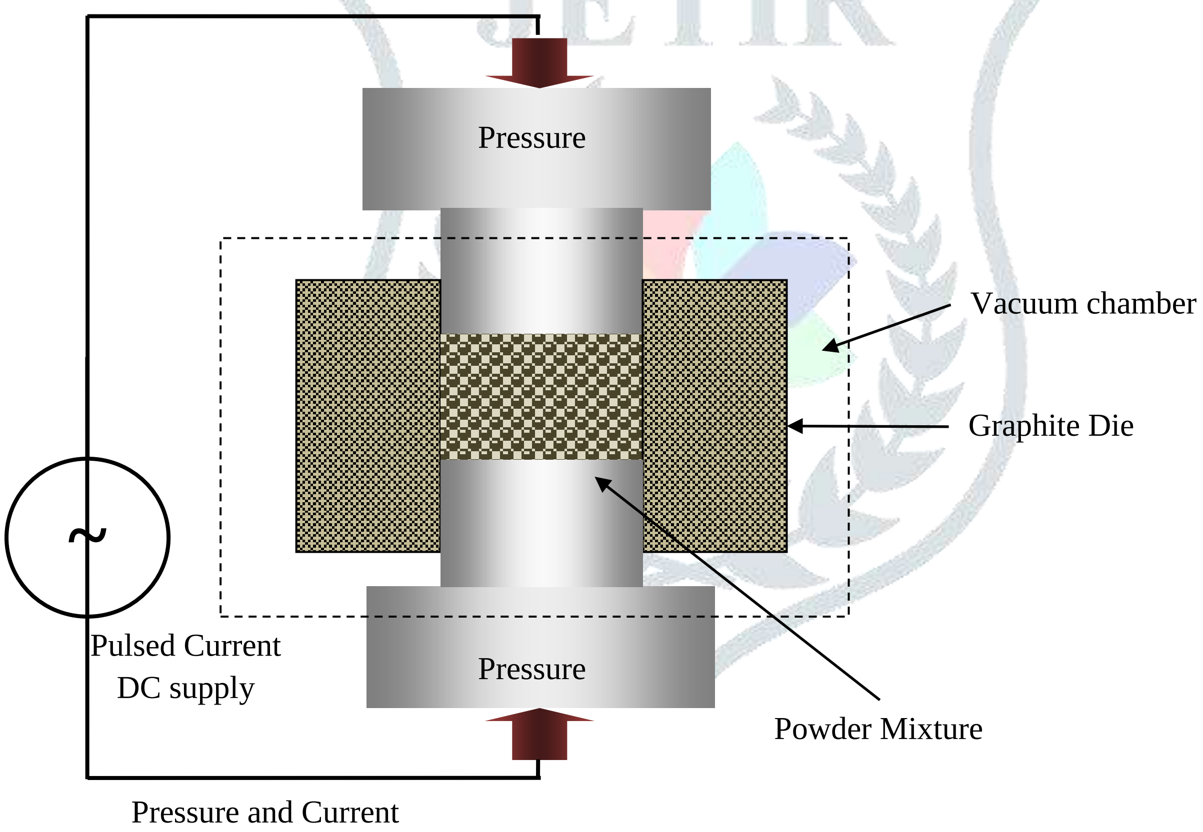

Figure 1.1. Schematic representation of SPS process

Spark plasma sintering (SPS) is performed in a Graphite die. The mechanical scheme of the process is similar to the Uniaxial (Die) Pressing. The load (commonly up to 100 MPa) is transferred to the powder through the upper punch. The pulsed DC power supply is connected to the upper and lower punches/electrodes. The process is conducted under either low pressure (vacuum) or inert gas atmosphere. Spark plasma sintering process is fast. Its overall duration is commonly 5-20 minutes. Since only surface layers of the powder particles are heated in the spark plasma sintering process, the average (monitored) temperature of the compact is relatively low: few hundred ºC lower than in conventional sintering process. The SPS procedure features a very high thermal efficiency because of the direct heating of the sintering graphite mold and stacked powder substances by means of the large spark pulse current. It can effortlessly consolidate a homogeneous, high-quality sintered compact because of the uniform heating, surface purification, and activation made viable with the aid of dispersing the spark factors.

2.2. Mechanism

The mechanism of the spark plasma sintering is still unclear therefore the process is also named as pulsed electric current sintering (PECS). However commercially the name SPS (spark plasma sintering) is more common. The most accepted mechanism of the pulsed electric current sintering (PECS) is based on the micro-spark discharge in the gap between powder particles. Vaporization, melting and sintering are completed in short periods of approximately 5 to 20 minutes, including temperature rise and holding times. The spark plasma sintering process proceeds through three stages namely Plasma heating, Joule heating and plastic deformation. Spark plasma sintering (SPS) technique is utilizing uniaxial force and a pulsed (on-off) direct electrical current (DC) under low atmospheric pressure to perform high speed consolidation of the powder particles. High-temperature plasma (spark plasma) momentarily generated inside the gaps between powder substances with the aid of electric discharge at the beginning of DC pulse energizing**.** The spark plasma sintering process proceeds through three stages namely Plasma heating, Joule heating and plastic deformation.

2.2.1. Plasma heating

The Spark plasma sintering (SPS) process inventors that the pulses generated sparks and even plasma discharges between the particle contacts, which were the reason that the processes were named, spark plasma sintering and plasma activated sintering. In the plasma heating process the electrical discharge between powder particles results in localized and momentary heating of the particles surfaces upto several thousand ºC. Since the micro-plasma discharges uniformly throughout the sample volume, the generated heat is also uniformly distributed. The particles surfaces are purified and activated due to the high temperature causing vaporization of the impurities concentrated on the particle surface.

2.2.2. Joule heating

At this stage, the pulsed direct electrical current (DC) flows from particle to particle and weld the particles under the mechanical pressure. The joule heat is generated by the electrical current. The strong joule heating effect at the particle conducting surface can often result in reaching the boiling point and therefore leads to fine grained powder surface. The joule heat increases the flow of the atoms/molecules in the necks increasing their growth.

2.2.3. Plastic deformation

The heated material becomes softer and it experiences plastic deformation under the uniaxial force. Plastic deformation combined with diffusion result in the densification of the powder compact to over 99% of its theoretical density.

Figure 2 shows the schematic representation of SPS technique. Figure 2 (a) shows the schematic representation of phenomenon of heat transfer and neck formation during SPS process. During SPS process thermal energy generated due to electrical sparks between the powder particles contact area. As a result of this partial melting of the grain boundary of powder, particle takes place and uniaxial applied pressure densified the powder mixture. This process of densification and solidification of the compact is known a sintering by SPS technique. Fig. 2(b) shows the mass transformation during the SPS process and also shows the phenomena of partial diffusion and welding of powder particles.

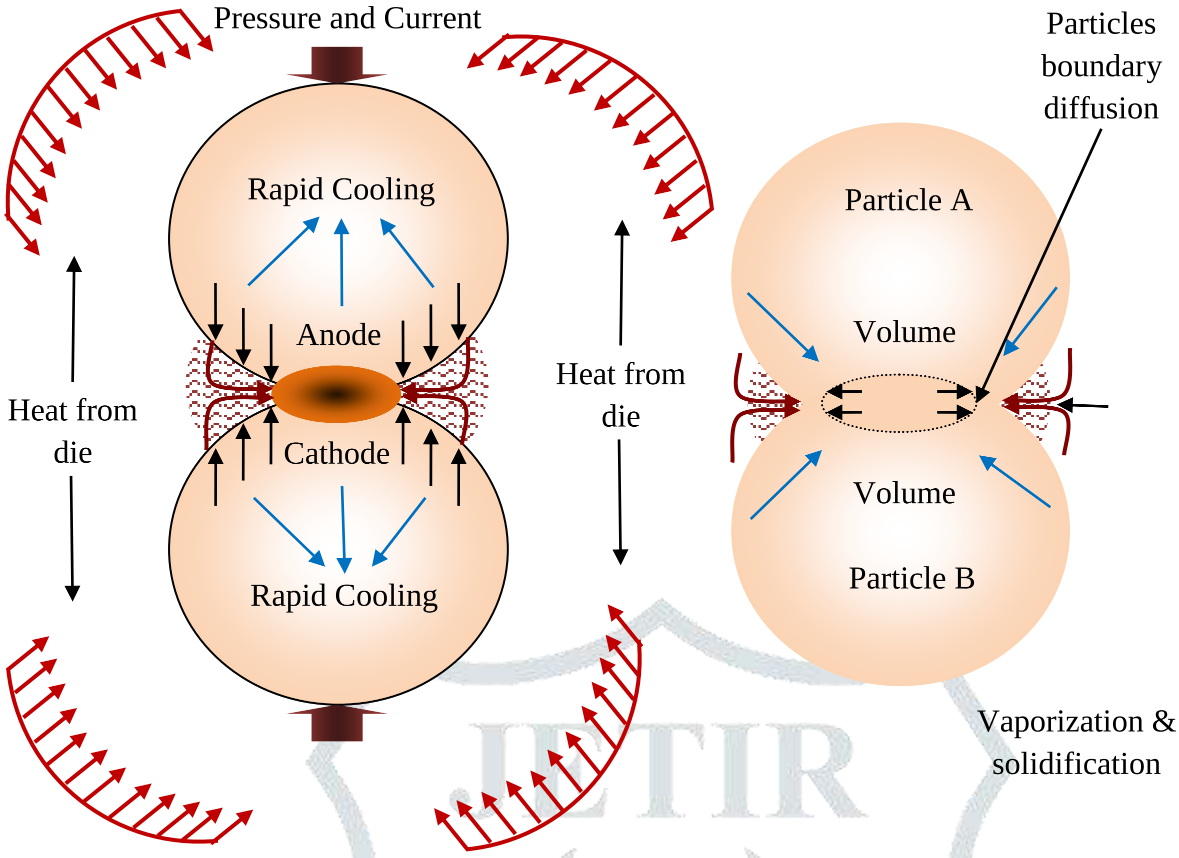

Fig. 3. (a) Schematic representation of SPS technique and (b-c) mechanism of sintering of powder particles during SPS

3. Current applications of SPS for the sintering of metallic alloys and composites for biomedical applications

Progressively in this direction, several metallic alloys/composites have been fabricated by the SPS technique for biomedical applications. The SPS technique has been accounted for a flexible and potential candidate to fabricate metallic and ceramic alloys and composites with improved mechano-biological properties and corrosion characteristic. The SPS technique was used for the fabrication of porous implants by optimizing its process parameters. The fabricated porous implant possessed desired bio-mechanical integrity required for the orthopaedic applications. Patra et al. fabricated nano-Y_2O_3 dispersed W-Ni-Mo and W-Ni-Ti-Nb composites by mechanical alloying and SPS technique. The sintering was performed at 1000 C, 1200 C and 1400 C for 5 min at 75 MPa pressure. The developed composite comprised high hardness, strength and wear resistance. Zhang et al. synthesized the high dense Ti-SiC-TiC composite by SPS technique uing titanium, graphite, and silicon powder particles. With the addition of TiC from 0–30 vol.%, the hardness and fracture toughness of the composites increase. The thermal conductivities of the composites were found to decrease with the increasing TiC volume content. The amorphous $Ti_{40}Zr_{10}Cu_{36}Pd_{14}$ powders (diameter<63 μm) with hydroxyapatite (HA) particles were mechanically alloyed to fabricate the Ti-based glassy/HA composite using SPS process. The effects of HA on the microstructure, thermal and mechanical properties of the as-fabricated composite was studied. With the increase in HA concentration, the glassy alloys are observed. Zhang et al. fabricated interconnected porous Ti-HA composite by SPS process and investigated the effect of HA content on the pore characteristics, mechanical properties and corrosion behaviour of the prepared samples. The results showed that with the increase of HA the density of developed sample decreases while the porosity increases. The compressive strength of porous Ti-HA decreased with increase of the HA content. The mechanical properties were decreased due to the combined effect of the pores characteristics. It was observed that porous Ti-(0–20%) HA bio composites exhibited higher load capacity but for Ti-30% HA the load capacity is decreased because of high porosity, large pore size. It could be concluded that the corrosion resistance of the porous Ti-HA samples decreased slightly with increasing the HA contents from 0 to 30 wt% [32]. Furthermore, Anawati et al. the bioactivity and corrosion resistance of SPS-synthesised Ti-40HA composite was studied. Results indicated that Ti composites containing 0–10% HA exhibited more corrosion resistance as compared to HA concentration of 20–30%. The developed composite possessed excellent bioactivity. He et al. studied the effect of HA content (0, 5, 10, 15 and 20 wt%) on the microstructure, mechanical properties and corrosion properties of the fabricated Ti-13Nb-13Zr-HAbased alloy. It was observed that HA concentration and relative density decrease with increase in HA content. Increasing the initial HA content to 5%, both the compression and yield strength increase but both decrease with further increase in HA content. Biocomposite with 10% of HA performed an optimal corrosion resistant in simulated artificial body fluid. Yang et. al. fabricated a biomedical alloy Ti-35Nb-7Zr-5Ta by mechanical alloying and spark plasma sintering at different sintering parameters. At a sintering Temperature of 1373K, the fabricated bulk alloys reached nearly full density. The micro hardness value of the as fabricated alloy is far larger than that of Ti-35Nb-7Zr-5Ta alloys fabricated by conventional powder metallurgy or hot wrought. The specific strength of the sintered alloy is relatively high. Sharma et. al. fabricated nano-porous β-type Ti-Nb alloy by spark plasma sintering process using powder metallurgical route for mechanical alloying of Ti and Nb powders. The Ti-Nb alloy exhibited low elastic modulus and high hardness (530 HV) at 1525 K of sintering temperature [33]. Zhang et. al. fabricated interconnected nano-porous Ti-HA biocomposite by spark plasma sintering process. It was reported that the SPS-prepared nano-porous Ti-HA biocomposite possessed not only low elastic modulus (8-15 GPa) but also exhibited high compressive strength (86-388 MPa) and also good bioactivity [34]. Hussein et. al. fabricated nano-grained Ti-Nb-Zr alloy using mechanical alloying and subsequent spark plasma sintering technique. The developed nano-structured alloy exhibited better microstructure and much high surface hardness (660 HV) as compared to the same alloy with other techniques [35]. Han et. al. fabricated Ti-Zr-Ni quasicrystalline alloys by spark plasma sintering technique and studied their mechanical properties such as micro-hardness, young's modulus, tensile, and compressive strength. It has been reported that the maximum micro-hardness, compression strength, the elastic deformation and Young modulus of the alloy was 7.03 GPa, (662 ± 50) MPa, 2.7 ± 0.1%, and (30 ± 3) GPa, respectively. The synthesized alloy also exhibited excellent wear resistance properties [36].

Till date no research study has reported the fabrication of Ti-28Nb-7Ta-5Zr-10HaP by combining powder metallurgical route for mechanical alloying of powders and spark plasma sintering technique. So, in the present research work the investigation on the fabrication of porous β-type (Ti-Nb-Ta-Zr-HaP) by spark plasma sintering process using powder metallurgical route are urgent needed for the next generation of implants. A comprehensive and critical investigation of the microstructure, morphology, phase composition, mechanical properties like micro-hardness and elastic modulus of the as-prepared alloys were conducted to evaluate the efficacy of SPS technique as a implant fabrication for preparing materials for biomedical applications [35-73].

2. CONCLUSIONS

Potential application of mechanical alloying and spark plasma sintering technique was considered for the design and development of new low elastic porous Mg-Zn-Mn-(HA-Si) composite with improved mechanical integrity, corrosion resistance properties and biocompatibility. Adequate amount of structural porosity ranging from 5-27% with average pore size >50µm was achieved in the as-sintered composites.The combined product of HA and Si primarily leads to the formation of biomimetic and biocompatible phases biomimetic oxide phases such as CaMg, $MgSi_2$, Mg-Zn, Mn-Si, SiO_2, Mn-CaO, Mn-P, Ca-Mn-O, ZnO_2, and CaMgSi in the porous layers, which enhanced the mechanical properties, corrosion resistance, and bioactivity of the as-sintered composites. Moreover, the combination of interconnected pore characteristics, low elastic modulus, high corrosion resistance and enhanced bioactivity might make porous Mg-Zn-Mn-(Si-HA) composites prepared by MA-SPS a promising candidate for Orthopaedic applications as screw, plates, and bio-inserts. The future work may focus on the control of the pore size, consistency and development of customized architectures in order to fulfill a wide range of applications. Along with this, clinical trials are also necessary for statistical analysis of in-vivo results are also necessary in order to meet up with all the claims.

REFERENCES

[1]. Niinomi, M., Nakai, M., & Hieda, J., 2012. Development of new metallic alloys for biomedical applications. Acta biomaterialia, 8(11), pp. 3888-3903.

[2]. Geetha, M., Singh, A. K., Asokamani, R., & Gogia, A. K., 2009. Ti based biomaterials, the ultimate choice for orthopaedic implants–a review. Progress in materials science, 54(3), pp. 397-425.

[3]. Bartolo, P., Kruth, J.P., Silva, J., Levy, G., Malshe, A., Rajurkar, K., Mitsuishi, M., Ciurana, J. and Leu, M., 2012. Biomedical production of implants by additive electro-chemical and physical processes. CIRP Annals-Manufacturing Technology, 61(2), pp.635-655.

[4]. Vaccaro, A.R., Singh, K., Haid, R., Kitchel, S., Wuisman, P., Taylor, W., Branch, C. and Garfin, S., 2003. The use of bioabsorbable implants in the spine. The Spine Journal, 3(3), pp.227-237.

[5]. Bártolo, P.J., Chua, C.K., Almeida, H.A., Chou, S.M. and Lim, A.S.C., 2009. Biomanufacturing for tissue engineering: present and future trends. Virtual and Physical Prototyping, 4(4), pp.203-216.

[6]. Prakash, C., Kansal, H.K., Pabla, B.S., Puri, S. and Aggarwal, A., 2016. Electric discharge machining–A potential choice for surface modification of metallic implants for orthopedic applications: A review. Proceedings of the Institution of Mechanical Engineers, Part B: Journal of Engineering Manufacture, 230(2), pp.331-353.

[7]. Prakash, C., Kansal, H.K., Pabla, B.S. and Puri, S., 2015. Processing and characterization of novel biomimetic nanoporous bioceramic surface on β-Ti implant by powder mixed electric discharge machining. Journal of Materials Engineering and Performance, 24(9), pp.3622-3633.

[8]. Prakash, C., Kansal, H.K., Pabla, B.S. and Puri, S., 2017. Experimental investigations in powder mixed electric discharge machining of Ti–35Nb–7Ta–5Zrβ-titanium alloy. Materials and Manufacturing Processes, 32(3), pp.274-285.

[9]. Prakash, C., Kansal, H.K., Pabla, B.S. and Puri, S., 2016. Multi-objective optimization of powder mixed electric discharge machining parameters for fabrication of biocompatible layer on β-Ti alloy using NSGA-II coupled with Taguchi based response surface methodology. Journal of Mechanical Science and Technology, 30(9), pp.4195-4204.

[10]. Prakash, C., Kansal, H.K., Pabla, B.S. and Puri, S., 2016. Powder mixed electric discharge machining: An innovative surface modification technique to enhance fatigue performance and bioactivity of β-Ti implant for orthopedics application. Journal of Computing and Information Science in Engineering, 16(4), p.041006.

[11]. Prakash, C. and Uddin, M.S., 2017. Surface modification of β-phase Ti implant by hydroaxyapatite mixed electric discharge machining to enhance the corrosion resistance and in-vitro bioactivity. Surface and Coatings Technology, 326, pp.134-145.

[12]. Niinomi, M. and Nakai, M., 2011. Titanium-based biomaterials for preventing stress shielding between implant devices and bone. International journal of biomaterials, 2011.

[13]. Spoerke, E.D., Murray, N.G., Li, H., Brinson, L.C., Dunand, D.C. and Stupp, S.I., 2005. A bioactive titanium foam scaffold for bone repair. Acta Biomaterialia, 1(5), pp.523-533.

[14]. Staiger, M.P., Pietak, A.M., Huadmai, J. and Dias, G., 2006. Magnesium and its alloys as orthopedic biomaterials: a review. Biomaterials, 27(9), pp.1728-1734.

[15]. Vahidgolpayegani, A., Wen, C., Hodgson, P. and Li, Y., 2017. Production methods and characterization of porous Mg and Mg alloys for biomedical applications. In Metallic Foam Bone, pp. 25-82.

[16]. Uddin, M.S., Hall, C. and Murphy, P., 2015. Surface treatments for controlling corrosion rate of biodegradable Mg and Mg-based alloy implants. Science and technology of advanced materials, 16(5), p.053501.

[17]. Cui, F.Z., Yang, J.X., Jiao, Y.P., Yin, Q.S., Zhang, Y. and Lee, I.S., 2008. Calcium phosphate coating on magnesium alloy for modification of degradation behavior. Frontiers of Materials Science in China, 2(2), pp.143-148.

[18]. Hassel T, Bach FW, and Krause C, 2007. Influence of alloy composition on the mechanical and electrochemical properties of binary Mg-Ca alloys and its corrosion behaviour in solutions at different chloride concentrations, Proc. 7th Int. Conf. Magnesium Alloys and Their Applications ed K U Kainer (Hoboken, NJ: Wiley), 2007, 789–95

[19]. Salahshoor, M. and Guo, Y.B., 2013. Process mechanics in ball burnishing biomedical magnesium–calcium alloy. The International Journal of Advanced Manufacturing Technology, 64(1-4), pp.133-144.

[20]. Uddin, M.S., Rosman, H., Hall, C. and Murphy, P., 2017. Enhancing the corrosion resistance of biodegradable Mg-based alloy by machining-induced surface integrity: influence of machining parameters on surface roughness and hardness. The International Journal of Advanced Manufacturing Technology, 90(5-8), pp.2095-2108.

[21]. Xu, L., Yu, G., Zhang, E., Pan, F. and Yang, K., 2007. In vivo corrosion behavior of Mg-Mn-Zn alloy for bone implant application. Journal of biomedical materials research Part A, 83(3), pp.703-711.

[22]. Li, Z., Gu, X., Lou, S. and Zheng, Y., 2008. The development of binary Mg–Ca alloys for use as biodegradable materials within bone. Biomaterials, 29(10), pp.1329-1344.

[23]. Xu, L., Zhang, E., Yin, D., Zeng, S. and Yang, K., 2008. In vitro corrosion behaviour of Mg alloys in a phosphate buffered solution for bone implant application. Journal of Materials Science: Materials in Medicine, 19(3), pp.1017-1025.

[24]. Zhang, E., Yin, D., Xu, L., Yang, L. and Yang, K., 2009. Microstructure, mechanical and corrosion properties and biocompatibility of Mg–Zn–Mn alloys for biomedical application. Materials Science and Engineering: C, 29(3), pp.987-993.

[25]. Zhang, E., He, W., Du, H. and Yang, K., 2008. Microstructure, mechanical properties and corrosion properties of Mg–Zn–Y alloys with low Zn content. Materials Science and Engineering: A, 488(1-2), pp.102-111.

[26]. Zhang EL, and Yang L, 2008. Microstructure, mechanical properties and bio-corrosion properties of Mg–Zn–Mn–Ca alloy for biomedical application. Mater. Sci. Eng. A, 497: 111–8.

[27]. Witte, F., Feyerabend, F., Maier, P., Fischer, J., Störmer, M., Blawert, C., Dietzel, W. and Hort, N., 2007. Biodegradable magnesium–hydroxyapatite metal matrix composites. Biomaterials, 28(13), pp.2163-2174.

[28]. Zhang, X., Wang, Z., Yuan, G. and Xue, Y., 2012. Improvement of mechanical properties and corrosion resistance of biodegradable Mg–Nd–Zn–Zr alloys by double extrusion. Materials Science and Engineering: B, 177(13), pp.1113-1119.

[29]. Gu, X.N., Li, N., Zheng, Y.F. and Ruan, L., 2011. In vitro degradation performance and biological response of a Mg–Zn–Zr alloy. Materials Science and Engineering: B, 176(20), pp.1778-1784.

[30]. Zhang, W., Li, M., Chen, Q., Hu, W., Zhang, W. and Xin, W., 2012. Effects of Sr and Sn on microstructure and corrosion resistance of Mg–Zr–Ca magnesium alloy for biomedical applications. Materials & Design, 39, pp.379-383.

[31]. Song, G., 2007. Control of biodegradation of biocompatable magnesium alloys. Corrosion science, 49(4), pp.1696-1701.

[32]. Zhang, S., Li, J., Song, Y., Zhao, C., Zhang, X., Xie, C., Zhang, Y., Tao, H., He, Y., Jiang, Y. and Bian, Y., 2009. In vitro degradation, hemolysis and MC3T3-E1 cell adhesion of biodegradable Mg–Zn alloy. Materials Science and Engineering: C, 29(6), pp.1907-1912.

[33]. T. Hassel, F.-W. Bach, A. Golovko, C. Krause, 2006. Magnesium technology in the grobal age, in: 45th Annual Conference of Metallurgists of CIM, Montreal, Quebec, Canada, pp. 359–370.

[34]. Li, N. and Zheng, Y., 2013. Novel magnesium alloys developed for biomedical application: a review. Journal of Materials Science & Technology, 29(6), pp.489-502.

[35]. Viswanathan, R., Rameshbabu, N., Kennedy, S., Sreekanth, D., Venkateswarlu, K., Sandhya Rani, M. and Muthupandi, V., 2013. Plasma electrolytic oxidation and characterization of spark plasma sintered magnesium/hydroxyapatite composites. In Materials Science Forum (Vol. 765, pp. 827-831). Trans Tech Publications.

[36]. Khanra, A.K., Jung, H.C., Yu, S.H., Hong, K.S. and Shin, K.S., 2010. Microstructure and mechanical properties of Mg-HAP composites. Bulletin of Materials Science, 33(1), pp.43-47.

[37]. Gu, X., Zhou, W., Zheng, Y., Dong, L., Xi, Y. and Chai, D., 2010. Microstructure, mechanical property, bio-corrosion and cytotoxicity evaluations of Mg/HA composites. Materials Science and Engineering: C, 30(6), pp.827-832.

[38]. Ye, X., Chen, M., Yang, M., Wei, J. and Liu, D., 2010. In vitro corrosion resistance and cytocompatibility of nano-hydroxyapatite reinforced Mg–Zn–Zr composites. Journal of Materials Science: Materials in Medicine, 21(4), pp.1321-1328.

[39]. Sun, J.E., Chen, M., Cao, G., Bi, Y., Liu, D. and Wei, J., 2014. The effect of nano-hydroxyapatite on the microstructure and properties of Mg–3Zn–0.5 Zr alloy. Journal of Composite Materials, 48(7), pp.825-834.

[40]. Zhao, J., Yu, Z.M., Yu, K. and Chen, L.J., 2011. Biodegradable Behaviors of Mg-6% Zn-5% Hydroxyapatite Biomaterial. In Advanced Materials Research (Vol. 239, pp. 1287-1291). Trans Tech Publications.

[41]. <http://www.healingwithnutrition.com/mineral.htm>.

[42]. McCarty, M.F., 1997. Reported anti atherosclerotic activity of silicon may reflect increased endothelial synthesis of heparan sulfate proteoglycans. Medical hypotheses, 49(2), pp.175-176.

[43]. Sripanyakorn, S., Jugdaohsingh, R., Elliott, H., Walker, C., Mehta, P., Shoukru, S., Thompson, R.P. and Powell, J.J., 2004. The silicon content of beer and its bioavailability in healthy volunteers. British Journal of Nutrition, 91(3), pp.403-409.

[44]. Mabuchi, M., Kubota, K. and Higashi, K., 1996. Tensile strength, ductility and fracture of magnesium-silicon alloys. Journal of materials science, 31(6), pp.1529-1535.

[45]. Ben-Hamu, G., Eliezer, D. and Shin, K.S., 2008. The role of Mg2Si on the corrosion behavior of wrought Mg–Zn–Mn alloy. Intermetallics, 16(7), pp.860-867.

[46]. Ben-Hamu, G., Eliezer, D. and Shin, K.S., 2007. The role of Si and Ca on new wrought Mg–Zn–Mn based alloy. Materials Science and Engineering: A, 447(1-2), pp.35-43.

[47]. Bakhsheshi-Rad, H.R., Idris, M.H., Abdul-Kadir, M.R., Ourdjini, A., Medraj, M., Daroonparvar, M. and Hamzah, E., 2014. Mechanical and bio-corrosion properties of quaternary Mg–Ca–Mn–Zn alloys compared with binary Mg–Ca alloys. Materials & Design, 53, pp.283-292.

[48]. Zhang, S., Zhang, X., Zhao, C., Li, J., Song, Y., Xie, C., Tao, H., Zhang, Y., He, Y., Jiang, Y. and Bian, Y., 2010. Research on an Mg–Zn alloy as a degradable biomaterial. Acta biomaterialia, 6(2), pp.626-640.

[49]. Khalil, K.A. and Almajid, A.A., 2012. Effect of high-frequency induction heat sintering conditions on the microstructure and mechanical properties of nanostructured magnesium/hydroxyapatite nanocomposites. Materials & Design (1980-2015), 36, pp.58-68.

[50]. Sunil, B.R., Ganapathy, C., Kumar, T.S. and Chakkingal, U., 2014. Processing and mechanical behavior of lamellar structured degradable magnesium–hydroxyapatite implants. Journal of the mechanical behavior of biomedical materials, 40, pp.178-189.

[51]. Zheng, B., Ertorer, O., Li, Y., Zhou, Y., Mathaudhu, S.N., Tsao, C.Y. and Lavernia, E.J., 2011. High strength, nano-structured Mg–Al–Zn alloy. Materials Science and Engineering: A, 528(4-5), pp.2180-2191.

[52]. Lala, S., Maity, T.N., Singha, M., Biswas, K. and Pradhan, S.K., 2017. Effect of doping (Mg, Mn, Zn) on the microstructure and mechanical properties of spark plasma sintered hydroxyapatites synthesized by mechanical alloying. Ceramics International, 43(2), pp.2389-2397.

[53]. Zhang, E., Yang, L., Xu, J. and Chen, H., 2010. Microstructure, mechanical properties and bio-corrosion properties of Mg–Si (–Ca, Zn) alloy for biomedical application. Acta biomaterialia, 6(5), pp.1756-1762.

[54]. Liu, X., Sun, J., Zhou, F., Yang, Y., Chang, R., Qiu, K., Pu, Z., Li, L. and Zheng, Y., 2016. Micro-alloying with Mn in Zn–Mg alloy for future biodegradable metals application. Materials & Design, 94, pp.95-104.

[55]. Fu, J., Liu, K., Du, W., Wang, Z., Li, S. and Du, X., 2017, March. Microstructure and mechanical properties of the as-cast Mg-Zn-Mn-Ca alloys. In IOP Conference Series: Materials Science and Engineering (Vol. 182, No. 1, p. 012053). IOP Publishing.

[56]. Rudinsky, S., Hendrickx, P., Bishop, D.P. and Brochu, M., 2016. Spark plasma sintering and age hardening of an Al–Zn–Mg alloy powder blend. Materials Science and Engineering: A, 650, pp.129-138.

[57]. Tünçay, M.M., Muñiz-Lerma, J.A., Bishop, D.P. and Brochu, M., 2017. Spark plasma sintering and spark plasma upsetting of an Al-Zn-Mg-Cu alloy. Materials Science and Engineering: A, 704, pp.154-163.

[58]. Chen, H.B., Kai, T., Bin, Y. and ZHANG, J.S., 2009. Nanostructured Al-Zn-Mg-Cu alloy synthesized by cryomilling and spark plasma sintering. Transactions of Nonferrous Metals Society of China, 19(5), pp.1110-1115.

[59]. Cao, N.Q., Pham, D.N., Kai, N., Dinh, H.V., Hiromoto, S. and Kobayashi, E., 2017. In Vitro Corrosion Properties of Mg Matrix In Situ Composites Fabricated by Spark Plasma Sintering. Metals, 7(9), p.358.

[60]. Cao, N.Q., Narita, K., Kobayashi, E. and Sato, T., 2016. Evolution of the microstructure and mechanical properties of Mg-matrix in situ composites during spark plasma sintering. Powder Metallurgy, 59(5), pp.302-307.

[61]. Narita, K., Kobayashi, E. and Sato, T., 2016. Sintering Behavior and Mechanical Properties of Magnesium/β-Tricalcium Phosphate Composites Sintered by Spark Plasma Sintering. Materials transactions, 57(9), pp.1620-1627.

[62]. Cheng, Y., Cui, Z., Cheng, L., Gong, D. and Wang, W., 2017. Effect of particle size on densification of pure magnesium during spark plasma sintering. Advanced Powder Technology, 28(4), pp.1129-1135.

[63]. Queudet, H., Lemonnier, S., Barraud, E., Guyon, J., Ghanbaja, J., Allain, N. and Gaffet, E., 2017. One-step consolidation and precipitation hardening of an ultrafine-grained Al-Zn-Mg alloy powder by Spark Plasma Sintering. Materials Science and Engineering: A, 685, pp.227-234.

[64]. Ghasali, E., Alizadeh, M., Niazmand, M. and Ebadzadeh, T., 2017. Fabrication of magnesium-boron carbide metal matrix composite by powder metallurgy route: comparison between microwave and spark plasma sintering. Journal of Alloys and Compounds, 697, pp.200-207.

[65]. Knotek, V., Ekrt, O. and Vojtěch, D., 2017. Electrochemical hydriding of Mg–Ni alloys compacted by spark plasma sintering. International Journal of Hydrogen Energy, 42(37), pp.23908-23914.

[66]. Zhang, H., Zhao, Y., Yan, Y., Fan, J., Wang, L., Dong, H. and Xu, B., 2017. Microstructure evolution and mechanical properties of Mg matrix composites reinforced with Al and nano SiC particles using spark plasma sintering followed by hot extrusion. Journal of Alloys and Compounds, 725, pp.652-664.

[67]. Knotek, V., Ekrt, O., Michalcová, A. and Vojtěch, D., 2017. Electrochemical hydriding of nanocrystalline Mg-Ni-X (X= Co, Mn, Nd) alloys prepared by mechanical alloying and spark plasma sintering. Journal of Alloys and Compounds, 726, pp.787-795.

[68]. Oliver, W.C. and Pharr, G.M., 1992. An improved technique for determining hardness and elastic modulus using load and displacement sensing indentation experiments. Journal of materials research, 7(6), pp.1564-1583.

[69]. American Society for Testing and Materials, Annual Book of ASTM Standards, ASTM, Designation: G102-89, 1999.

[70]. Zheng, R., Ma, F., Xiao, W., Ameyama, K. and Ma, C., 2017. Achieving enhanced strength in ultrafine lamellar structured Al2024 alloy via mechanical milling and spark plasma sintering. Materials Science and Engineering: A, 687, pp.155-163.

[71]. Cullity BD, 1957. Elements of X-Ray Diffraction, American Journal of Physics, 25, pp 394.

[72]. Zhang, L., He, Z.Y., Zhang, Y.Q., Jiang, Y.H. and Zhou, R., 2016. Rapidly sintering of interconnected porous Ti-HA biocomposite with high strength and enhanced bioactivity. Materials Science and Engineering: C, 67, pp.104-114.

[73]. Jamesh, M., Kumar, S. and Narayanan, T.S., 2012. Electrodeposition of hydroxyapatite coating on magnesium for biomedical applications. Journal of Coatings Technology and Research, 9(4), pp.495-502.